Spectral features of the quasielastic line in amorphous solids and supercooled liquids: A detailed low-frequency Raman scattering study

S. N. Yannopoulos[1,*] and D. Th. Kastrissios[1,2]
[1]*Foundation for Research and Technology Hellas–Institute of Chemical Engineering and High Temperature Chemical Processes, P.O. Box 1414, GR-26500 Patras, Greece*
[2]*Department of Chemical Engineering, University of Patras, GR-26500, Patras, Greece*
(Received 31 May 2001; revised manuscript received 4 October 2001; published 25 January 2002)

The spectral features of the quasielastic light scattering in amorphous solids and supercooled liquids are investigated through a combined Stokes and antiStokes low-frequency Raman scattering study. Emphasis is given on the specific spectral details of the quasielastic line rather than on elucidating its microscopic origin. Our approach is quite general since it includes glass formers with a strong, an intermediate, and a fragile dynamic character. The results suggest that the quasielastic contribution is a symmetric spectral feature around the laser line. This finding makes possible the separation of the quasielastic line and the Boson peak. It further raises certain skepticism concerning reduction schemes followed up in the literature for the analysis of low-frequency Raman data and for models that combine these two contributions. The limiting ($\omega \rightarrow 0$) behavior of the product of the vibrational density of states and the Raman coupling coefficient has also been extracted. The validity of some phenomenological approaches is also discussed in light of the experimental facts presented in this paper and some suggestions are being advanced.

DOI: 10.1103/PhysRevE.65.021510 PACS number(s): 64.70.Pf, 78.30.Ly

I. INTRODUCTION

Numerous aspects of structural glasses have been the subject of strong debate in the recent past. A typical example is the elucidation of the low-frequency modes of amorphous solids as revealed through light [1] or neutron [2] scattering investigations, where currently there exists no consensus. Whether or not specific properties related to structural and/or dynamic effects in this case follow universal laws is still doubtful [3,4].

The lack of an accurate description of the spectral features of the scattered light (e.g., intensity, polarization, temperature dependence of the various components, etc.) in the low-energy region appears to be due to two reasons. First, to the limited amount of glass-forming materials frequently used in experimental studies in order to establish universalities; as a consequence, universalities are being settled on an incomplete basis. And second, to the usual practice (in theoretical approaches to spectral line shapes) of adopting elements from approaches that treat different problems. As a result, the proposed analyses, although conforming to specific experimental data, are frequently devoid of a general physical transparency. These models are, therefore, not capable of accurately describing a broader range of experimental data for a number of glass-forming materials.

Up until now, it is widely admitted that the low-frequency Raman spectrum consists of two main contributions: (i) the vibrational part or the so-called Boson peak (BP) whose intensity follows the temperature dependence of the Bose factor, $n(\omega,T)=[\exp(\hbar\omega/k_BT)-1]^{-1}$, and (ii) the quasi-elastic (QE) component usually assigned to the presence of very fast (subpicosecond) relaxation processes. The origin of the Boson peak has been the subject of numerous works, sometimes with self-contradictory views as can be evidenced through the available literature, and will not be pursued here. On the other hand, much less attention has been paid to the QE line and especially to its spectral form. The QE line was registered for the first time more than 25 yr ago by Winterling, who tried also to provide arguments for its explanation [5]. At that time, Theodorakopoulos and Jäckle assigned QE light scattering to structurally relaxing two-state defects [6]. Quite recently, the spectral shape of the fast relaxations in glassy silica has been investigated, the conclusion being that thermally activated transitions in double-well potentials suffice to account for the experimental data [7]. It is the aim of the present paper to try to clarify some obscure points related to this issue. To this goal, we have undertaken a low-frequency Raman scattering study in which we record both the Stokes and anti-Stokes regions in order to check the symmetry properties around $\omega=0$ of the quasielastically scattered light.

To keep our approach general enough, we have chosen to include in our investigation a ''strong,'' an ''intermediate,'' and a ''fragile'' glass former [8] and to carry out the analysis at temperatures where either the Boson peak or the QE contribution dominate. In particular, we have investigated As_2O_3, $ZnCl_2$, and $2BiCl_3-KCl$ whose low-frequency modes have been analyzed in Refs. [9], [3], and [10], respectively.

This paper is organized as follows. In Sec. II, a brief account of the experimental procedure is given. Section III contains a short theoretical background to facilitate the subsequent discussion and solid reasoning concerning the invalidity of the proposed first-order reduction schemes for the QE line. The data analysis procedure is provided in Sec. IV. Our results are presented in detail in Sec. V, followed by a discussion related to their impact on the current phenomenological status of the field. Finally, the most important conclusions drawn from the present study are summarized in Sec. IV.

*Corresponding author. Electronic address: sny@iceht.forth.gr

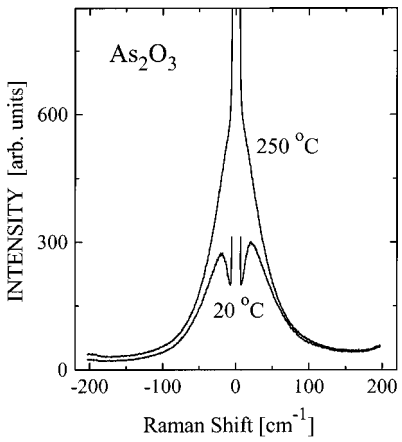

FIG. 1. Stokes and anti-Stokes depolarized (HV) Raman spectra for As_2O_3 at temperatures below and above the glass transition temperature, $T_g \approx 160\,°C$. The spectra are the average of seven accumulations in order to enhance the signal-to-noise ratio.

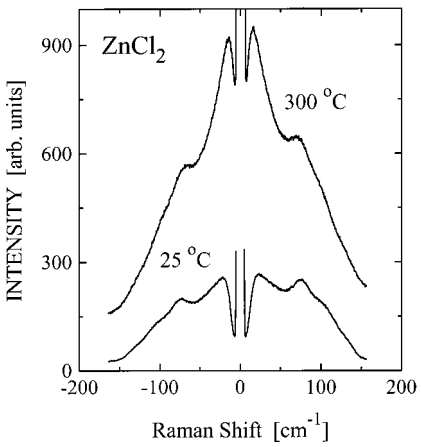

FIG. 2. Stokes and anti-Stokes depolarized (HV) Raman spectra for $ZnCl_2$ at temperatures below and above the glass transition temperature, $T_g \approx 102\,°C$. The spectra are the average of seven accumulations in order to enhance the signal-to-noise ratio.

II. EXPERIMENTS

The raw materials were purchased from various companies and were subsequently purified by special sublimation techniques in order to meet the high-quality demands for accurate spectroscopic measurements. It is well known that inorganic and, in particular, halide glasses are easily affected by humidity and oxygen. This shortcoming can be overcome if the entire treatment procedure is carried out in an inert-gas-filled glove box. Details for the purification procedure of the chemicals and the specimen preparation for As_2O_3 ($T_g \approx 160\,°C$ and $T_m \approx 312\,°C$), $ZnCl_2$ ($T_g \approx 102\,°C$ and $T_m \approx 318\,°C$,) and $2BiCl_3$-KCl ($T_g \approx 37\,°C$ and $T_m \approx 167\,°C$) may be found in Refs. [9], [3], and [10], respectively.

Right-angle spectra were recorded by a 0.85 m double monochromator (Spex 1403). The excitation source was an Ar^+ laser operating with an output power of between 50–150 mW depending on the material. The instrumental resolution was fixed at 1.0 cm^{-1} for the whole set of measurements and the temperature was controlled within ± 1 K. Both scattering geometries, polarized VV and depolarizaed HV, were employed and a calibration procedure with the aid of a Hg lamp was frequently taking place during spectra accumulation in order to correct for possible drifts of the monochromator's gratings. The error in the wave-number range is thus estimated to be less than 0.2 cm^{-1}. Stokes and anti-Stokes Raman spectra were recorded in one run with the aid of a mechanical flag used to block the elastic peak when the interval $-4-+4$ cm^{-1} was scanned. Spectra were accumulated repeatedly until the signal-to-noise ratio reached a satisfactory level. Highly smooth spectra are of critical importance in the analysis due to the fact that we deal with the Stokes and anti-Stokes difference as explained in Sec. IV. The averaged depolarized spectra for As_2O_3, $ZnCl_2$, and $2BiCl_3-KCl$ are shown in Figs. 1, 2, and 3, respectively.

III. THEORETICAL CONSIDERATIONS

It should be instructive to mention briefly some general aspects of the field that will be useful for the subsequent discussion. In the current literature the Boson peak and the QE contribution have been treated in the spirit of two main guidelines, namely, the *superposition* and the *convolution* (or coupling) approach. According to the former, the composite low-frequency spectrum consists of the sum of the two components, whilst the latter relies on the assumption that relaxators cannot scatter light directly but they couple to vibrational modes modifying their spectrum. Ample argumentation in favor of the superposition model has been recently presented in view of new experimental data [3,10] and from a recent detailed study that has shown the applicability of the double-well potential picture in describing fast relaxations for both strong and fragile systems at least up to 310 K. [7].

The spectral form of the first-order (harmonic approximation) vibrational part, namely, the Boson peak, has been described by Shuker and Gammon [11] through the relation

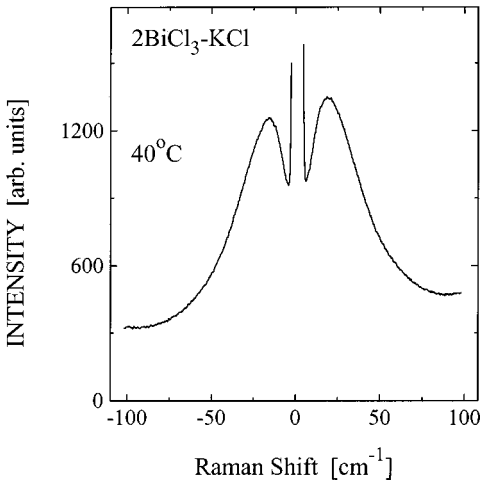

FIG. 3. Stokes and anti-Stokes depolarized (HV) Raman spectra for $2BiCl_3-KCl$ very close to the glass transition temperature, $T_g \approx 37\,°C$. The spectra are the average of seven accumulations in order to enhance the signal-to-noise ratio.

$$I^{\alpha\beta}(\omega)=C^{\alpha\beta}(\omega)g(\omega)\omega^{-1}\left[n(\omega)+\begin{vmatrix}1\\0\end{vmatrix}\right], \tag{1}$$

where $C^{\alpha\beta}(\omega)$ is the photon-phonon (Raman) coupling coefficient that denotes the ability of a vibrational mode to scatter light and $g(\omega)$ is the vibrational density of states. The superscript $\alpha\beta$ denotes particular polarization geometries. The expression in the square brackets represents the Bose factor correction for the Stokes $[n(\omega)+1]$ and anti-Stokes $[n(\omega)]$ regions of the spectrum.

Eq. (1) formed the basis for the introduction of various reduction schemes. To isolate the function $g(\omega)$, the reduced Raman intensity and the susceptibility form $\chi^n(\omega)$ defined as

$$I^{\alpha\beta}_{\rm red}(\omega)=\frac{I^{\alpha\beta}(\omega)}{\omega[n(\omega,T)+1]}, \tag{2a}$$

$$\chi''(\omega)=\frac{I^{\alpha\beta}(\omega)}{[n(\omega,T)+1]} \tag{2b}$$

are introduced. Although such reduction schemes are predominantly valid for the vibrational part of the spectrum, they are frequently used also to reduce the relaxational contribution; for the latter, however, neither an analogous ''relaxational density of states'' nor a ''photon-relaxator'' coupling coefficient can be apparently conceived, let alone to be defined.

It is the objective of the present paper to examine the validity of such a reduction scheme to the QE region of the spectrum. At first glance, it does not seem to be obvious at all why such a central spectral line, assigned mainly to very fast relaxational processes originating from local density fluctuations, should obey Bose statistics. It should be seen instead as a ''classical'' type of light scattering contrasted to the quantum nature accompanying the inelastically scattered light by vibrational modes. This idea is further supported by an analogous case, namely, the spectral form of the so-called ''Mountain mode'' [12,13]. Although near the glass transition temperature the Mountain peak is much narrower than the QE peak observed in the low-frequency Raman spectrum, at higher temperatures—where the structural relaxation time becomes of the order of ~1 ps—the Mountain peak broadens considerably becoming comparable even to the QE contribution. However, the Mountain mode is successfully described as a symmetric one, although it attains the same degree of ''quasielastic'' character (~0.5 THz) with the QE line at high temperatures.

To put the above discussion in a more rigorous guise let us discuss the fundamental origin of the difference between the first-order Stokes (I^S) and anti-Stokes ($I^{\rm aS}$) scattered intensities. It can be rather easily proven that I^S and $I^{\rm aS}$ are related through the well-known *detailed balance* equation [14],

$$\left(\frac{I^{\rm aS}}{I^S}\right)^{\rm 1st}=\frac{n(\omega)}{[n(\omega)+1]}. \tag{3}$$

We have omitted here for simplicity the λ^4 correction factor, which has been taken into account in the data analysis. Although the above equation is a general result, there are cases where detailed balance breaks down [15]. This happens when the equations describing the scattering process do not obey the *time reversal symmetry* [15,16], and such an example is the case of scattering that is not caused by the discrete vibrational energy levels but instead originates from density fluctuations (relaxational mode). When energy dissipation is taken into account, fluctuations have been shown to be irreversible [17], leading, therefore, to violation of the detailed balance condition.

Moreover, it should be reminded here that the factor $n(\omega)$ is the average occupation number of phonons at thermodynamic equilibrium for a system that consists of *simple harmonic oscillators* [18]. The much stronger temperature dependence that the QE line intensity exhibits—as compared to that predicted by the Bose factor for first-order scattering—renders the use of Eqs. (2) superficial as far as the reduction of the relaxational mode observed in the lower part of the spectrum is concerned. In fact, the temperature dependence of the QE line is more akin to the second-order scattering mechanism. In the case of second-order vibrational scattering, the right hand side in Eq. (3) is replaced by the factor $n(\omega)[n(\omega)-1]/[n(\omega)+1][n(\omega)+2]$ that implies a much more pronounced depletion of the anti-Stokes intensity as compared to the Stokes one. Specifically, at room temperature for first-order scattering, $(I^{\rm aS}/I^S)^{\rm 1st}\approx 0.95$ at $\omega=10\ {\rm cm}^{-1}$, while for second-order scattering at the same frequency $(I^{\rm aS}/I^S)^{\rm 2nd}\approx 0.82$. Whereas the 5% difference in the former may be considered to be within the experimental noise, in the latter, the ~20% contrast between I^S and $I^{\rm aS}$ should be clearly observed in the experimental spectra. However, as is immediately seen from Figs. 1, 2, and 3, the intensities of the Stokes and anti-Stokes minima below the Boson peak, which characterize the relaxational behavior, appear almost equal at first sight; they further turn out to be equal, within the experimental error, after being analyzed according to the method proposed in the Sec. IV. Concluding, proper care must be taken as regards what is *true* Raman (vibrational) signal; QE scattering can not be strictly considered as a Raman scattering mechanism.

Before closing this section it should be instructive to recall some already known ideas concerning the relaxational part that will help make the connection between the aforementioned arguments and the data analysis that follows. It is well known [13] that in the classical limit $\hbar\omega\ll k_BT$ the scattered intensity related to some relaxational mode is an even function of frequency. Moreover, when dealing with classical liquids the van Hove correlation function is purely real and hence the dynamic structure factor $S(\omega)$ is an even function of ω [13]. It is also known that the susceptibility is related to the dynamic structure factor or, equivalently, to the scattered intensity through the celebrated fluctuation-dissipation theorem, $\chi''_{\rho\rho}(\omega)=-\pi\rho(\omega/k_BT)S(\omega)$ as long as the linear response regime is valid, where the subscript ρ denotes density fluctuations. The above equation is also found in the equivalent form $\chi''_{\rho\rho}(\omega)=(\omega/2k_BT)S(\omega)$. What eventuates from the above discussion is that susceptibilities that represent a kind of reduced spectra involve factors proportional to the quantity ω/k_BT; the latter is proportional to the first term in the Bose factor series expansion. However, the full expres-

sion of the Stokes side Bose factor and its first term in the series expansion differ by almost 10% at 50 cm^{-1}; a difference that cannot be considered as negligible. In the Sec. IV we propose a procedure that is able to provide a disentanglement of the two main low-energy contributions avoiding any reduction schemes concerning the relaxational part of the spectrum.

IV. DATA ANALYSIS PROCEDURE

Let us consider that the total low-frequency scattered intensity can be written as a sum of a symmetric part $R(\omega,T)$ representing all zero centered modes and the asymmetric vibrational contribution $[n(\omega,T)+1]V(\omega)$ or $[n(\omega,T)]V(\omega)$ for the Stokes and anti-Stokes sides, respectively. Then, one can express the total scattered intensity in these two regions as

$$I^{S}_{\mathrm{exp}}(\omega,T)=R(\omega,T)+[n(\omega,T)+1]V(\omega), \tag{4a}$$

$$I^{\mathrm{aS}}_{\mathrm{exp}}(\omega,T)=R(\omega,T)+n(\omega,T)V(\omega), \tag{4b}$$

where $R(\omega,T)$ contains also a thermal factor. The advantage of this scheme is that no specific form for the thermal factor needs to be assumed.

As is easily discerned from the above equations, the ''pure'' vibrational spectrum, free of any other contributions and thermal effects, can be obtained through the expression,

$$V(\omega)=I^{S}(\omega,T)-I^{\mathrm{aS}}(\omega,T), \tag{5}$$

which after a multiplication with the $[n(\omega,T)+1]$ factor can yield back the Stokes component of the scattered intensity originating solely from the first-order vibrational contribution. That is,

$$I^{S}_{\mathrm{BP}}(\omega,T)=V(\omega)[n(\omega,T)+1], \tag{6}$$

which allows us to obtain the symmetric part through the difference

$$R(\omega,T)=I^{S}_{\mathrm{exp}}(\omega,T)-I^{S}_{\mathrm{BP}}(\omega,T). \tag{7}$$

Equation (7) is another form of Eq. (4a).

The above arguments imply that if the assumption of a symmetric central part is correct, as put forward in Eqs. (4), then the excess scattering will not show up in the plot of the intensity as described by Eq. (6), and the following approximation should hold,

$$\lim_{\omega\to 0} I^{S}_{\mathrm{BP}}(\omega,T)\to 0. \tag{8}$$

The last relation simply states that the vibrational part of the light scattering spectrum has to vanish at zero wave number.

V. RESULTS AND DISCUSSION

To give an example of the sensitivity of the method just described, in Fig. 4(a) we plot theoretical Stokes low-frequency spectra for a symmetric (solid line) and an asymmetric (dashed line) QE line. These spectra have originated from the same anti-Stokes spectrum; however, in the asymmetric case both Boson peak and QE have been scaled with the Bose factor while in the symmetric one only the Boson peak has followed the Bose scaling. Then, by using Eqs. (5) and (6) we have calculated the quantity I^{S}_{BP} shown in Fig. 4(b). It is easily seen that in the case of a symmetric QE line the condition (8) is fulfilled while, obviously, this is not the case for the spectrum computed from the asymmetric QE line. It is noteworthy that even a small difference in the lineshapes of the symmetric and asymmetric spectra [region around the minimum in Fig. 4(a)] brings about a huge dissimilarity in the $\omega\to 0$ limit of the $I^{S}_{\mathrm{BP}}(\omega,T)$ spectrum. An even larger dissimilarity would have been observed if the Stokes-side QE line had been constructed by a factor incorporating a temperature dependence closer to that described by the second-order scattering mechanism.

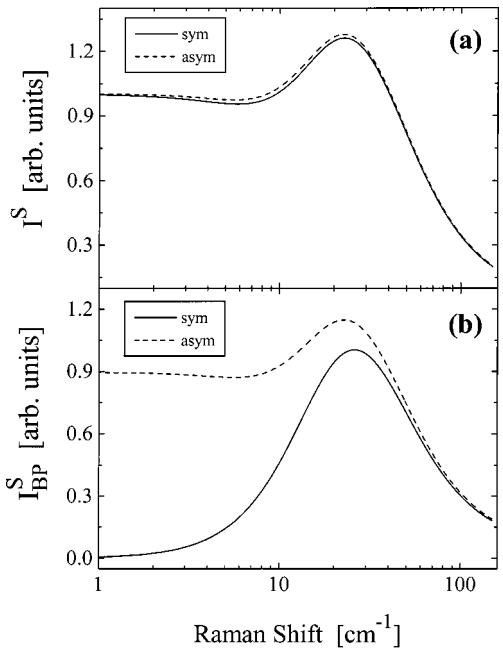

FIG. 4. (a) Semilogarithmic plot of theoretically calculated Stokes side low-frequency Raman spectra obtained as a superposition of BP and QE contributions for symmetric (solid curve) and asymmetric QE lines (dashed curve). These spectra have originated from the same anti-Stokes spectrum; however, in the asymmetric case both BP and QE have been scaled with the Bose factor while in the symmetric one only the BP has followed the scaling. (b) Semilogarithmic plot of ''pure'' Boson peak spectra, corresponding to the spectra of (a), obtained through Eqs. (5) and (6). The spectra show that in the presence of asymmetry the limiting low-frequency behavior ($\omega\to 0$) is very different compared to that of the symmetric case.

Let us now apply the reasoning mentioned in the preceding section to the raw spectra illustrated in Figs. 1, 2, and 3. As can be seen from these plots, we have chosen to measure spectra at temperatures for which the strength of the QE contribution compared to that of the Boson peak (revealed through the depth of the minimum below the Boson peak maximum) varies from almost negligible (when $T\ll T_g$) to dominant (when $T>T_g$).

The $I^{S}(\omega,T)-I^{\mathrm{aS}}(\omega,T)$ spectra have been obtained and

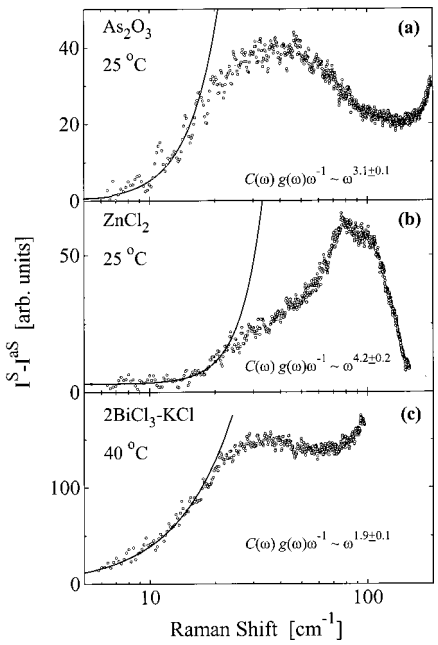

FIG. 5. Semilogarithmic plot of the reduced $[I^S(\omega,T) - I^{aS}(\omega,T)]$ depolarized Raman spectra (open circles) for (a) As_2O_3, (b) $ZnCl_2$, and (c) $2BiCl_3-KCl$. The solid lines represent power law fits to the data corresponding up to the maximum of the BP as described in the text.

are illustrated in Fig. 5 for the lowest temperatures. This figure reveals the following facts. First, the limiting low-frequency spectra do not show remnants of the QE component providing a first indication that it is rather a symmetric line; this will become clear in the subsequent discussion. Second, the frequency dependence of the Raman coupling coefficient can be elucidated. Indeed, by combining Eqs. (1) and (4) and considering the QE line as symmetric we obtain

$$I^S(\omega,T) - I^{aS}(\omega,T) = C^{\alpha\beta}(\omega) g(\omega) \omega^{-1} \propto \omega^x. \qquad (9)$$

We have introduced a power law dependence in the above equation and tried to obtain the overall exponent x. The high-frequency cutoffs of the fitting procedure used were at about 20 cm^{-1} for all glasses studied. The resulting values for the power law exponent do not show any common or universal behavior, in particular, $x(As_2O_3) = 3.1 \pm 0.1$, $x(ZrCl_2) = 4.2 \pm 0.2$, and $x(2BiCl_3\text{-}KCl) = 1.9 \pm 0.1$. Accordingly, the exponent for the net $C^{\alpha\beta}(\omega)g(\omega)$ product assumes mean values close to 4, 5, and 3 for As_2O_3, $ZnCl_2$, and $2BiCl_3$-KCl, respectively. The frequency dependence of the Raman coupling coefficient has been so far indirectly determined through the comparison of neutron and Raman scattering data leading often to self-contradictory conclusions (see, for example, Ref. [4] for a recent short review). In our case, based on the rigid conception that at such very low frequencies the vibrational density of states follows fairly well the Debye law, i.e., $g(\omega) \propto \omega^2$, we are led to the outcome that the low-frequency behavior of the Raman coupling coefficient follows a power law with exponents close to 2, 3, and 1 for As_2O_3, $ZnCl_2$, and $2BiCl_3-KCl$, respectively.

Let us now discuss the physical implications of the x values extracted above for the different materials. From the theoretical point of view, studies on orientationally disordered crystals [19] and slightly damped acoustic phonons [1] have resulted to an ω^2 dependence of the Raman coupling coefficient. On the other hand, linear, ''sublinear,'' and ''overlinear'' dependencies are common in experimental works [4]. Therefore, the quadratic or linear frequency dependence found for As_2O_3 and $2BiCl_3-KCl$ glasses are not unusual in the current literature. As regards $ZnCl_2$, it is not possible at present to decide if the somehow unexpected high value of the exponent is indeed correct or due to an inaccurate estimation of the $C^{\alpha\beta}(\omega)$ frequency dependence for this material from the low-lying opticlike vibrational modes (located at about 75 cm^{-1}). At least, what becomes evident from the above analysis is that the Raman coupling coefficient does not exhibit any common frequency dependence among various glass-forming liquids, as is usually stated. Actually, this is not at all surprising since the coupling coefficient is a very specific material property related to the way that vibrational motion modulates the polarizability of the medium and as such it has to differ among supercooled liquids.

Proceeding one step beyond, we have attempted to reconstruct the corresponding Stokes side BP spectra from the pure vibrational parts of the spectra (or reduced spectra), i.e., $I^S(\omega,T) - I^{aS}(\omega,T)$, by using Eq. (6). The results obtained for all the depolarized measured spectra are depicted in Figs. 6, 7, and 8 by the open circles, for As_2O_3, $ZnCl_2$ and $2BiCl_3-KCl$, respectively. It is obvious that in all cases the noise of the reconstructed spectra is much higher than that of the raw data that are also shown in the figures for comparison. However, all reconstructed spectra share a common feature: they seem to follow rather well the predictions of Eq. (8). Alternatively, the light scattering vibrational spectrum tends to almost zero intensity as $\omega \to 0$. This observation provides a clear evidence for the validity of our initial assumption concerning the symmetric nature of the QE component. Indeed, based on the message given by Fig. 5, we expect that even traces of asymmetry, see Fig. 4(a), would result in nonvanishing values of the intensity when approaching the zero frequency; obviously, this is not the case in Figs. 6, 7, and 8. This supports the conception that the correction of the quasielastic light scattering through the Bose factor, which is valid only for the first-order vibrational modes, is meaningless from the physical point of view and might be misleading when trying to formulate theories and/or phenomenological models.

As a further advantage of the approach employed in this paper, one can calculate the QE component through Eq. (7). After subtracting the pure vibrational spectra, $I^S_{BP}(\omega,T)$ from the Stokes side experimental data we have obtained the QE spectra (open circles) for the materials under study, shown in Fig. 9 at the lowest measured temperature for each glass. Lorentzian lineshapes have been used to fit the spectral form of the QE contribution and are plotted as solid lines in Fig. 9. It is evident that the Lorentzian line fits nicely to the experimental data resulting to physically acceptable values for the

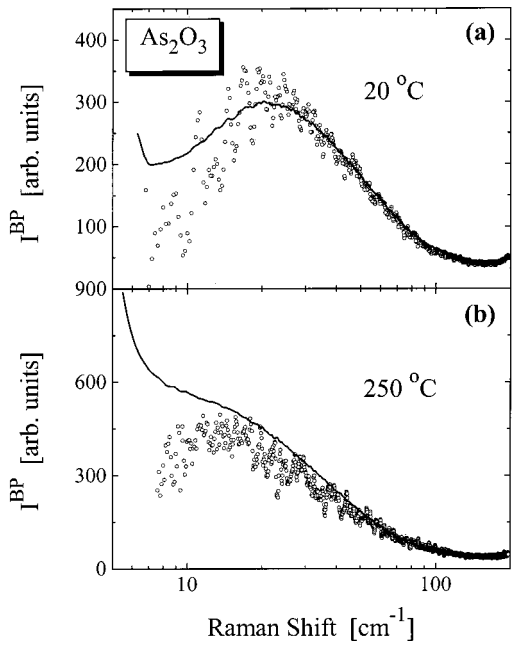

FIG. 6. Semilogarithmic plot of the depolarized ''pure'' Boson peak spectra (open circles) for As_2O_3 in the glassy (a) and the high-temperature supercooled state (b). The Stokes-side raw spectra are also plotted for comparison.

full widths, namely, $\sim 24\ cm^{-1}$, $\sim 30\ cm^{-1}$, and $\sim 10\ cm^{-1}$ for As_2O_3, $ZnCl_2$, and $2BiCl_3$-KCl, respectively.

A comment should be made here concerning the determination of the QE component from the low-frequency Raman spectra. In particular, in some approaches, the following idea is adopted [20]. A spectrum is measured at very low tempera-

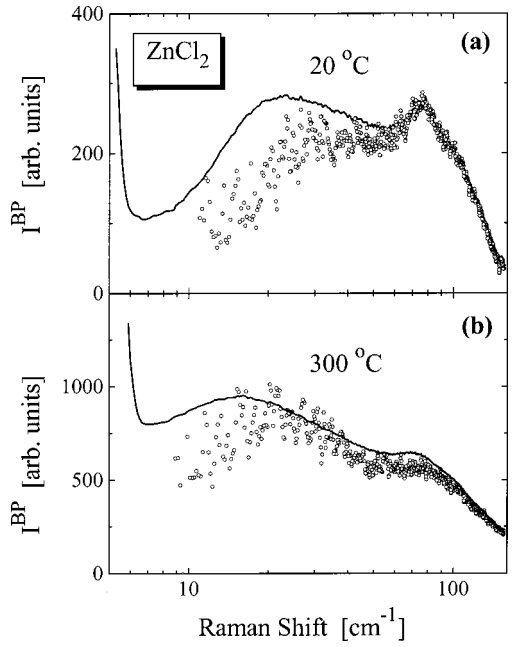

FIG. 7. Semilogarithmic plot of the depolarized ''pure'' Boson peak spectra (open circles) for $ZnCl_2$ in the glassy (a) and the high-temperature supercooled state (b). The Stokes-side raw spectra are also plotted for comparison.

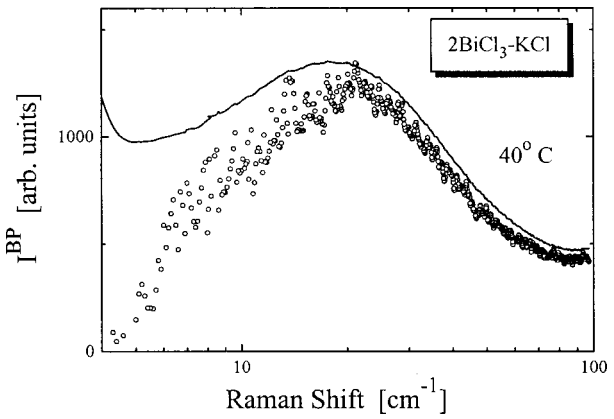

FIG. 8. Semilogarithmic plot of the depolarized ''pure'' Boson peak spectrum (open circles) for $2BiCl_3-KCl$ near the glass transition temperature. The Stokes-side raw spectrum is also plotted for comparison.

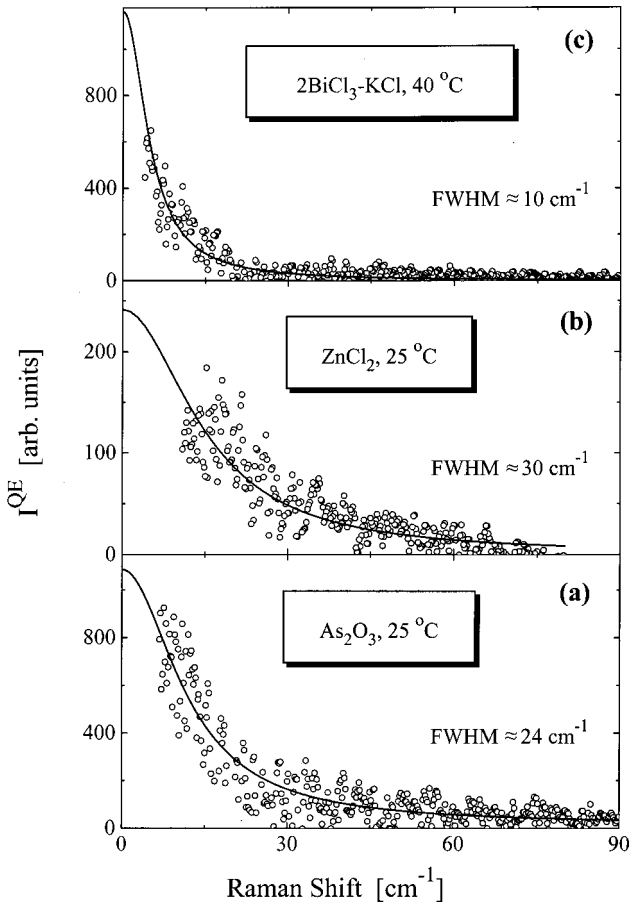

FIG. 9. Pure quasielastic contribution (open circles) for (a) As_2O_3, (b) $ZnCl_2$, and (c) $2BiCl_3-KCl$ obtained after subtracting the BP from the raw spectra. The solid lines represent Lorentzian fits to the QE spectra with fullwidths at half maximum 24 cm^{-1}, 30 cm^{-1}, and 10 cm^{-1} for As_2O_3, $ZnCl_2$, and $2BiCl_3-KCl$, respectively.

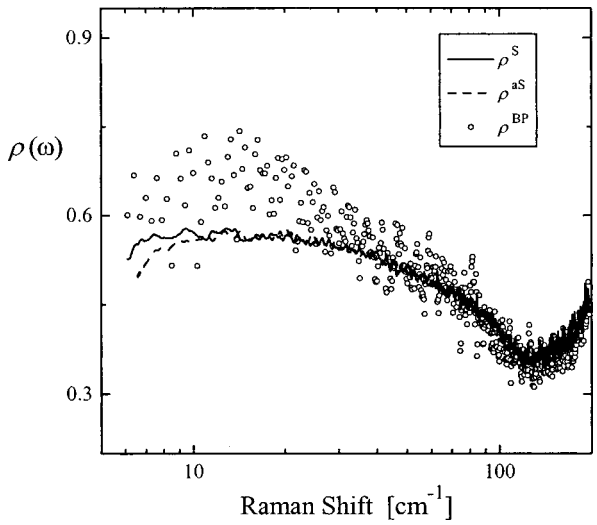

FIG. 10. Semilogarithmic plot of the Stokes (solid line), anti-Stokes (dashed line), and Boson peak (open circles) depolarization ratio obtained from the 20 °C polarized and depolarized spectra of As_2O_3.

tures, where the relaxational or QE contribution is negligible and the spectrum represents only the vibrational contribution. Then, the properly Bose-scaled low-temperature spectrum is subtracted from any high-temperature spectrum resulting to the pure QE part. However, such a method is not indisputable since it ignores (i) the effects of the temperature-dependent anharmonicity implicit to the Boson peak vibrations and (ii) the fact that the spectral form (effective width) of the Boson peak might be temperature dependent. On the contrary, the approach that we are currently suggesting that is based on the comparison between Stokes and anti-Stokes spectra, although more laborious, seems to be a better candidate for an accurate determination of the spectral form of the QE scattering since no one assumption is invoked.

A frequently overlooked parameter of the light scattering intensities, namely, the depolarization ratio $\rho(\omega)$ can provide valuable information for the issues treated in this work. The depolarization ratio is defined as the ratio between the depolarized (HV) and polarized (VV) scattered intensities. The idea is as follows. One should reasonably expect that the depolarization ratio in the Stokes $\rho^S(\omega)$ and the anti-Stokes $\rho^{aS}(\omega)$ sides to be the same if the Bose scaling was valid for the total spectrum, i.e., vibrational and relaxational contribution. On the other hand, if the QE component does not follow Bose scaling, and remains symmetric, we would expect to observe a deviation between $\rho^S(\omega)$ and $\rho^{aS}(\omega)$ especially at very low frequencies. This region cannot be close to zero frequency since, by definition, the difference between Stokes and anti-Stokes vanishes in this region. Evidently, the maximum difference lies in the frequency range of the minimum formed below the BP maximum, as is also evident from Fig. 4(a). Indeed, plotting together the depolarization ratios for the Stokes and anti-Stokes parts for As_2O_3, Fig. 10, we observe a clear dissimilarity between $\rho^S(\omega)$ and $\rho^{aS}(\omega)$ below ~ 10 cm^{-1}. This is an indication that the Stokes and anti-Stokes parts of the QE line are related by a different factor than that relating the corresponding intensities for the Boson factor. The ''pure'' Boson peak depolarization ratio $\rho^{BP}(\omega)$ is also plotted for comparison. It should be stressed here that this is the first time where the depolarization ratio of the ''pure'' Boson peak is presented. Partial depolarization ratios have been also calculated in Ref. [10], however extracted from fitting procedures. The knowledge of the ''pure'' BP depolarization ratio is of crucial importance for testing theoretical predictions. Finally, it should be mentioned that we have proceeded to the calculation of $\rho(\omega)$ only in the case of As_2O_3 since in that case we have the most reliable spectra in both scattering geometries.

It is interesting to compare our results with a recently published related work [21(a)]. It has been stated in this work [21(a)] that in the case of direct light scattering the total spectrum can be considered as the sum of relaxational and vibrational contributions. On the contrary, when QE scattering can be phonon mediated the experimental spectrum is not the sum of the two contributions. However, the authors of Ref. [21(a)] undertake a substraction procedure and conclude that their result agrees better with the phonon-mediated model in the framework of which a subtraction of the two contributions is meaningless. They have based their conclusion on the argument that the high-frequency wing of the susceptibility form of the QE line—obtained after the subtraction of the vibrational part—decays much faster than the decay predicted by the direct light scattering mechanism. However, their treatment has been based on a number of assumptions. First, the intensity is arbitrarily extrapolated at low frequencies with different power laws for different glasses. Second, the estimation of the Boson peak softening at high temperatures is unavoidably subjected to errors. But the most important approximation, that strongly affects the form of the high-frequency wing decay, is the unjustified choice of the frequency range in which the spectra have been forced to overlap. The authors have chosen to overlap the spectra in the interval 600–3000 GHz. For the mentioned reason, the high-frequency susceptibility wing vanishes above the cut-off frequency $\omega \approx 600$ GHz for silica and $\omega \approx 850$ GHz for the lithium borate glass. The choice of a higher frequency, above which the spectra are forced to overlap, would render the high-frequency wing decay slower.

The aforementioned discussion shows that the result obtained by the subtraction scheme of Ref. [21(a)] is inadequate since it is vitally influenced by the procedure details. Above all, the vanishing of the QE line at frequencies around 20 cm^{-1} for silica and 28 cm^{-1} for the lithium borate glass, contradicts the findings of Ref. [21(b)] where its half-width is of the order of 15 cm^{-1} and 20 cm^{-1} for the mentioned glasses, respectively.

Closing this section it is worth mentioning that an attempt analogous to the one undertaken here has appeared some years ago by Zwick and Landa (ZL) [22]. In that work the authors did not find positive indications for the symmetry of the QE line. However, ZL have selected to study three liquids, namely, dioxane, water, and glycerol at room temperature where a Boson peak is not clearly present, and the QE intensity and some other central modes, are the main contributions in the spectrum. Their conclusions have been drawn

after comparing Stokes and anti-Stokes spectra in the frequency range 400–400 cm^{-1}, while they did not focus in the region of interest, i.e., below 50 cm^{-1}. Further, the spectra of ZL were not at the level of accuracy (resolution, possible shift corrections, etc.) to provide unequivocally information on the symmetry properties of the QE line.

VI. CONCLUDING REMARKS

A detailed low-frequency Raman scattering investigation has been undertaken in order to elucidate the spectral features of the quasielastic line. To keep our approach general we have chosen to examine three inorganic glass-formers characterized by dynamic behavior ranging from strong to fragile. Measurements at various temperatures, when possible, have been conducted so as to pass from the regime where vibrational dynamics prevail to that where relaxational processes dominate. Qualitative arguments are being presented in Sec. III to justify why this central contribution has to be a symmetric line around $\omega=0$, suggesting criteria for a quantitative description.

The results obtained for all studied systems indicate that the QE component is a symmetric line, which does need to be treated under the same temperature basis as the Boson peak. The advantage of this finding is that one can separate the QE line part or any other symmetric contribution (including constant unwanted background) from the ''pure'' vibrational contribution. As a consequence, the limiting $\omega\rightarrow 0$ behavior of the net $C^{\alpha\beta}(\omega)g(\omega)$ product has been determined for the three glasses studied in this work. Finally, the observed dissimilarity between $\rho^{S}(\omega)$ and $\rho^{aS}(\omega)$ at low frequencies also supports the fact that the ratio of the Stokes and anti-Stokes QE intensities is different than the respective ratio of the Boson peak.

The outcome of this paper supports the validity of the superposition model that treats the total low-frequency spectrum as a sum of the relaxational and the vibrational contribution. On the contrary, in the convolution (or coupling) approach the two mentioned components are interrelated and treated under the same reduction scheme. It is also worth mentioning that experimental evidence has been recently presented through inelastic neutron scattering supporting the idea that the fast relaxation processes in supercooled liquids have to be envisaged as a first, fast stage of the primary or α relaxation [23]. This is another support of the idea adopted here that the picosecond dynamics originate from fast (local) structural rearrangements being therefore differentiated from the Bose-scaled vibrational spectrum.

ACKNOWLEDGMENTS

S.N.Y. acknowledges financial support from the General Secretariat of Research and Technology, Hellas in the framework of the PENED/99EΔ44 grant.

[1] J. Jäckle in *Amorphous Solids: Low-Temperature Properties*, edited by W. A. Phillips (Springer, Berlin, 1981) p. 151.
[2] U. Buchenau, M. Prager, N. Nücker, A. J. Dianoux, N. Ahmad, and W. A. Phillips, Phys. Rev. B **34**, 5665 (1986).
[3] S. N. Yannopoulos and G. N. Papatheodorou, Phys. Rev. B **62**, 3728 (2000).
[4] S. N. Yannopoulos, J. Chem. Phys. **113**, 5868 (2000).
[5] G. Winterling, Phys. Rev. B **12**, 2432 (1975).
[6] N. Theodorakopoulos and J. Jäckle, Phys. Rev. B **14**, 2637 (1976).
[7] J. Wiedersich, N. V. Surovstev, V. N. Novikov, E. Rössler, and A. P. Sokolov, Phys. Rev. B **64**, 064207 (2001).
[8] The terms ''strong'' and ''fragile'' supercooled liquids have been coined by Angell [C. A. Angell, J. Non-Cryst. Solids **131-133**, 15 (1991)] in order to distinguish between supercooled liquids that the temperature dependence of their dynamic variable, i.e., viscosity or structural relaxation time, follows an Arrhenius dependence (strong) or substantially non-Arrhenius form (fragile). Naturally, when the deviation from the Arrhenius behavior is moderate the term ''intermediate'' is frequently employed.
[9] S. N. Yannopoulos, G. N. Papatheodorou, and G. Fytas, J. Chem. Phys. **107**, 1341 (1997).
[10] S. A. Kirillov and S. N. Yannopoulos, Phys. Rev. B **61**, 11 391 (2000).
[11] R. Shuker and R. Gammon, Phys. Rev. Lett. **25**, 222 (1970).
[12] B. J. Berne and R. Pecora, *Dynamic Light Scattering* (Wiley, New York, 1976); J. P. Boon and S. Yip, *Molecular Hydrodynamics* (Dover, New York, 1991).
[13] J. P. Hansen and I. McDonald, *The Theory of Simple Liquids* (Academic Press, London, 1986).
[14] L. D. Landau and E. M. Lifshitz, *Electrodynamics of Continuous Media*, 2nd ed. (Pergamon, New York, 1984).
[15] W. Hayes and R. Loudon, *Scattering of Light by Crystals* (Wiley, Brisbane, 1978); R. Loudon, J. Raman Spectrosc. **7**, 10 (1978).
[16] W. Heitler, *The Quantum Theory of Radiation* (Dover, New York, 1984).
[17] A. G. Sitenko, Phys. Lett. A **282**, 43 (2001).
[18] G. Burns, *Solid State Physics* (Academic, San Diego, 1990).
[19] E. Whalley and J. E. Bertie, J. Chem. Phys. **46**, 1264 (1967).
[20] See for example, F. Terki, C. Levelut, J. L. Prat, M. Boissier, and J. Pelous, J. Phys.: Condens. Matter **9**, 3955 (1997).
[21] (a) V. N. Novikov, N. V. Surovtsev, and S. Kojima, J. Chem. Phys. **115**, 5278 (2001); (b) V. N. Novikov, Phys. Rev. B **58**, 8367 (1998).
[22] A. Zwick and G. Landa, J. Raman Spectrosc. **25**, 849 (1994).
[23] M. Russina, F. Mezei, R. Lechner, S. Longeville, and B. Uban, Phys. Rev. Lett. **84**, 3630 (2000).